



OPEN

Non-invasive liver fibrosis markers are increased in obese individuals with non-alcoholic fatty liver disease and the metabolic syndrome

Anders Askeland^{1,2}, Rikke Wehner Rasmussen¹, Mimoza Gjela^{1,3}, Jens Brøndum Frøkjær^{2,3}, Kurt Højlund⁴, Maiken Mellergaard^{1,2,5} & Aase Handberg^{1,2,5}✉

The need for early non-invasive diagnostic tools for chronic liver fibrosis is growing, particularly in individuals with obesity, non-alcoholic fatty liver disease (NAFLD), and the metabolic syndrome (MetS) since prevalence of these conditions is increasing. This case-control study compared non-invasive liver fibrosis markers in obesity with NAFLD and MetS (NAFLD-MetS, $n=33$), in obese ($n=28$) and lean ($n=27$) control groups. We used MRI (T1 relaxation times (T1) and liver stiffness), circulating biomarkers (CK18, PIIINP, and TIMP1), and algorithms (FIB-4 index, Forns score, FNI, and MACK3 score) to assess their potential in predicting liver fibrosis risk. We found that T1 (892 ± 81 ms vs. 818 ± 64 ms, $p < 0.001$), FNI ($15 \pm 12\%$ vs. $9 \pm 7\%$, $p = 0.018$), CK18 (166 ± 110 U/L vs. 113 ± 41 U/L, $p = 0.019$), and MACK3 (0.18 ± 0.15 vs. 0.05 ± 0.04 , $p < 0.001$) were higher in the NAFLD-MetS group compared with the obese control group. Moreover, correlations were found between CK18 and FNI ($r = 0.69$, $p < 0.001$), CK18 and T1 ($r = 0.41$, $p < 0.001$), FNI and T1 ($r = 0.33$, $p = 0.006$), MACK3 and FNI ($r = 0.79$, $p < 0.001$), and MACK3 and T1 ($r = 0.50$, $p < 0.001$). We show that liver fibrosis markers are increased in obese individuals with NAFLD and MetS without clinical signs of liver fibrosis. More studies are needed to validate the use of these non-invasive biomarkers for early identification of liver fibrosis risk.

Keywords Obesity, Non-alcoholic fatty liver disease, The metabolic syndrome, Obesity phenotype, Non-invasive biomarkers, Liver fibrosis risk

Non-alcoholic fatty liver disease (NAFLD) affects more than half of all obese individuals, why it is one of the most common disorders associated with obesity¹. The prevalence of obesity is steadily increasing worldwide^{2,3}, along with elevated frequency of NAFLD and its pathological progression⁴. Moreover, the negative health impact of obesity is linked to various elements of the metabolic syndrome (MetS) including central obesity, hypertension, dyslipidaemia, and elevated glucose levels⁵.

NAFLD encompasses several hepatic pathological changes, ranging from simple steatosis (excessive liver fat) to non-alcoholic steatohepatitis (NASH, characterized by liver cell injury and inflammation), liver fibrosis, cirrhosis, and ultimately, hepatocellular carcinoma^{4,6,7}. The progression of NAFLD is a continuum that is closely linked to the development of liver fibrosis, which is considered the most critical histological predictor of mortality in NAFLD patients⁸. Consequently, early identification of obese individuals with liver fibrosis risk is essential to mitigate its development and improve prognosis⁹.

At present, liver biopsy is the gold standard for identifying liver fibrosis. However, this is prone to sampling errors and severe complications such as bleeding and mortality, excluding its use for screening purposes in large populations^{10,11}. As such, several non-invasive methods have been explored as promising alternatives. Some well-established non-invasive methods for advanced liver fibrosis include transient elastography (FibroScan) and

¹Department of Clinical Biochemistry, Aalborg University Hospital, Aalborg, Denmark. ²Department of Clinical Medicine, Aalborg University, Aalborg, Denmark. ³Department of Radiology, Aalborg University Hospital, Aalborg, Denmark. ⁴Steno Diabetes Center Odense, Odense University Hospital, Odense, Denmark. ⁵Maiken Mellergaard and Aase Handberg contributed equally to this work. ✉email: aaha@rn.dk

the fibrosis-4 index (FIB-4 index)^{12,13}. In addition, certain novel techniques are showing promise. For instance, magnetic resonance imaging (MRI)-based techniques enables evaluation of liver fibrosis by assessment of T1 relaxation time (T1 mapping) and liver stiffness by magnetic resonance elastography (MRE)^{14–16}. Additionally, circulating biomarkers have been proposed to indirectly measure liver fibrosis. These include tissue inhibitor of metalloproteinases 1 (TIMP1) that play a key role in the progression of liver fibrosis, procollagen-III peptide (PIIINP) associates with extracellular matrix (ECM) remodelling during liver fibrogenesis, and cytokeratin-18 (CK18) fragments are released from apoptotic hepatocytes and involved in the promotion of fibrosis^{17–20}. Finally, a variety of algorithms have been developed, such as the Forns score, fibrosis non-alcoholic steatohepatitis index (FNI), and the MACK3 score that incorporate several aspects of developing fibrosis^{21–24}. Most studies have focused on class III obesity, selected fibrosis markers, or advanced fibrosis and fibrotic NASH^{25–30}.

Obesity is a complex and heterogeneous condition that presents varying degrees of metabolic comorbidities. Several studies discuss the concept of “obesity phenotypes” to distinguish between obese individuals who appear metabolically healthy and those with metabolic comorbidities (metabolically unhealthy)^{31,32}. As such, stratification of obese individuals based on metabolic risk (i.e. with/without NAFLD and MetS) has been proposed to improve clinical management, ultimately to limit obesity and NAFLD progression as well as reducing or reversing the development of liver fibrosis³². Previous findings showed that the presence of MetS associated with high risk of NASH and fibrosis determined by liver biopsy³³. This is particularly interesting, considering the recent recommendations by Rinella et al. to replace the term NAFLD with metabolic dysfunction-associated steatotic liver disease (MASLD) that comprehend both NAFLD and MetS parameters. While NAFLD alone is defined by a spectrum of steatosis and pathophysiology in the liver that is not related to alcohol consumption, MASLD encompasses both NAFLD and one cardiometabolic risk factor³⁴. As this study (MULTISITE study) focuses on NAFLD and MetS, with MetS defined as the presence of three cardiometabolic risk factors (described in detail in “Methods” section). We have thus, following recent recommendations, included data grouped and analysed according to this new MASLD terminology to offer comparability. This adds invaluable insight into the differences between these definitions and potential inherent challenges. However, since the MULTISITE study was designed and conducted prior to these recommendations, we find it necessary to maintain and primarily focus on the original grouping characteristics.

To the best of our knowledge, no studies have assessed a broad range of non-invasive fibrosis biomarkers in obese individuals with NAFLD and MetS (NAFLD-MetS) or MASLD. We hypothesize that obese individuals with both NAFLD and MetS or MASLD but without clinical signs of progressing liver fibrosis exhibit elevated levels of non-invasive biomarkers of liver fibrosis. Thus, the objective of this study was to assess a broad range of liver fibrosis markers in obese individuals to determine potential early onset/risk of liver fibrosis. We thus assessed early liver fibrosis by MRI (T1 mapping and MRE), circulating biomarkers (TIMP1, CK18, and PIIINP), and risk algorithms (FIB-4 index, FNI, Forns, and MACK3) in obese NAFLD-MetS or MASLD, an obese control group, and a lean control group.

Results

Study participants

A total of 98 participants who met the inclusion criteria were included in the study. Out of these, 88 individuals were subject to investigation, including 27 lean control individuals, 28 obese control individuals, and 33 individuals with obesity and NAFLD-MetS (Fig. 1). When grouping according to the MASLD criteria the study included 27 lean control individuals, 25 obese control individuals, and 36 individuals with obesity and MASLD (Fig. S1).

Clinical and metabolic characteristics

When comparing clinical features between the groups, the female to male ratio was comparable between the groups (obese NAFLD-MetS: 18/15; obese control: 22/6; lean control: 18/15; $p=0.104$, Table 1). Moreover, levels of liver enzymes were comparable in the lean (ALT: 23.0 ± 12 U/L and AST: 21.5 ± 5.0 U/L) and obese control groups (ALT: 22.4 ± 10.2 U/L and AST: 22.2 ± 6.1 U/L), while both were elevated in the obese NAFLD-MetS group (ALT: 33.8 ± 16 U/L, $p=0.003$ and AST: 25.4 ± 7.3 U/L, $p=0.05$, Table 1). Homeostatic model for assessment of insulin resistance (HOMA-IR) differed between all three groups with the highest level in the obese NAFLD-MetS group (3.4 ± 1.5) and decreased in the control groups (obese: 1.6 ± 0.5 ; lean: 0.8 ± 0.4 , $p<0.001$, Table 1). Ethnicity was similar among the groups (data not shown). Similar clinical distributions were observed when grouping according to the MASLD criteria (Table S1). Finally, as expected according to the study design, liver steatosis determined by MRI was significantly higher in the obese NAFLD-MetS group (13%), compared with control groups: obese (3%) and lean (2%) (Table 1 and Fig. S2a). This was similar when grouping according to MASLD (Table S1 and Fig. S2b).

Liver fibrosis biomarkers

Several non-invasive biomarkers of liver fibrosis differed between study groups. In terms of MRI, there were differences in T1 relaxation times (ANOVA <0.001) and MRE measuring liver stiffness (ANOVA = 0.033, Table S2). When analysing circulating biomarkers, we saw differences in CK18 (ANOVA <0.001 , Table S2). Finally, investigating fibrosis algorithms revealed differences in the Forns score (ANOVA = 0.001), the FIB-4 index (ANOVA = 0.033), FNI (ANOVA <0.001), and MACK3 (ANOVA <0.001 , Table S2).

Regarding T1 mapping and liver stiffness, the post-hoc analysis showed that T1 relaxation times were significantly higher in the obese NAFLD-MetS group compared with the obese control group (892 ± 81 ms vs. 818 ± 64 ms, $p<0.001$) and when compared with the lean control group (892 ± 81 ms vs. 787 ± 61 ms, $p<0.001$; Fig. 2a). Conversely, the lean control individuals had significantly higher liver stiffness compared with the

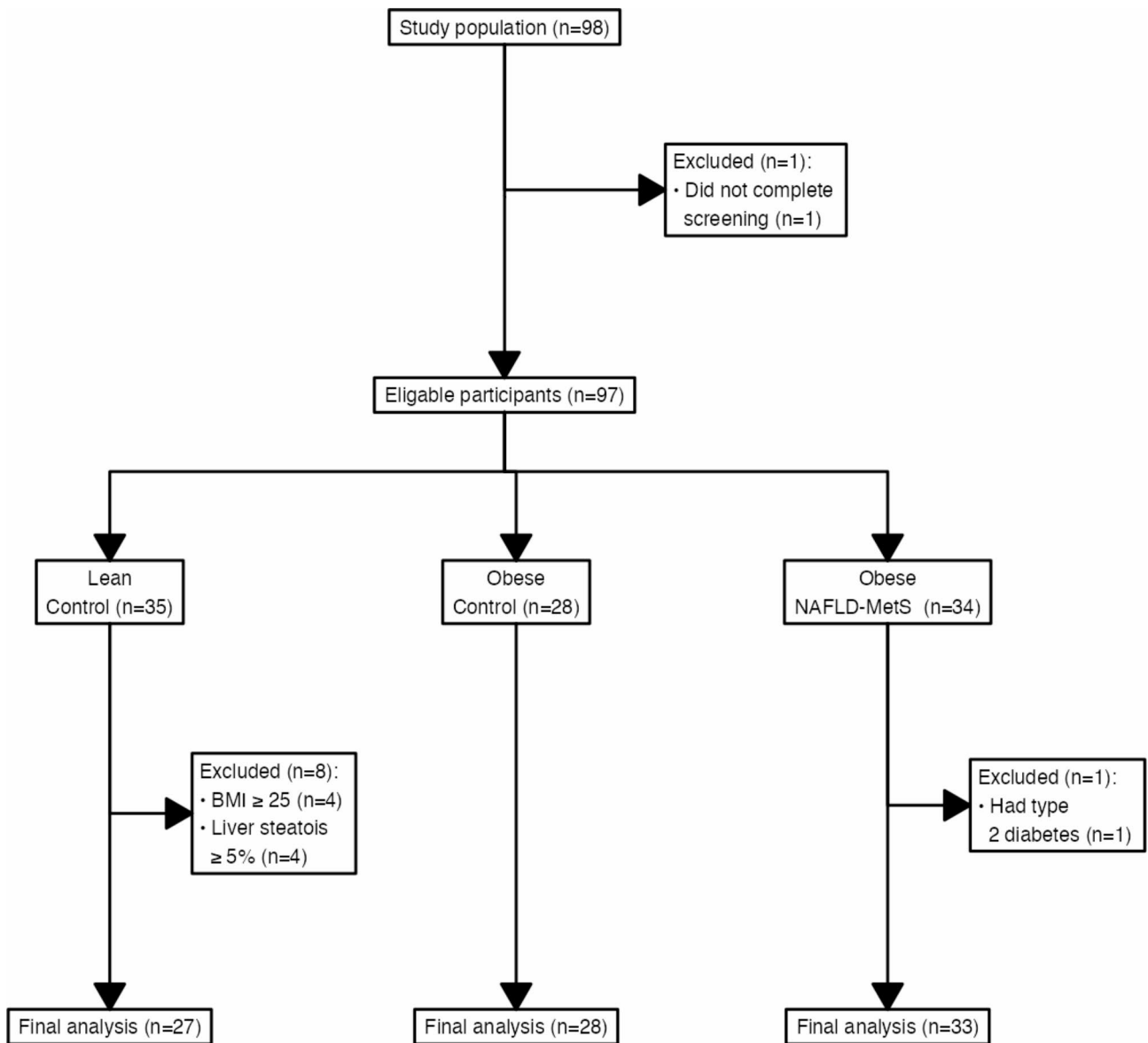


Fig. 1. Flow chart (consort diagram) showing the study population as (1) Lean control group, (2) Obese control group, and (3) Obese NAFLD-MetS group. The flow chart further shows the number of participants that were screened and found eligible as participants to be included in final data analysis as well as information on participants that were excluded.

obese NAFLD-MetS group (2.4 ± 0.4 kPa vs. 2.1 ± 0.4 kPa, $p = 0.029$) and when compared with the obese control individuals (2.4 ± 0.4 kPa vs. 2.2 ± 0.3 kPa, $p = 0.040$; Fig. 2b).

Examining the relationship between T1 relaxation times, liver stiffness, and liver steatosis revealed strong correlation of T1 relaxation times with liver steatosis ($r = 0.71$, $p \leq 0.001$; Fig. 3a) while liver stiffness had a medium correlation ($r = -0.32$, $p = 0.007$; Fig. 3b). This association was strongest in the obese NAFLD-MetS group, where T1 relaxation time ($r = 0.77$, $p \leq 0.001$; Fig. 3c) and liver stiffness ($r = -0.38$, $p = 0.047$; Fig. 3d) correlated with liver steatosis. All imaging data were similar when grouping according to the MASLD criteria (Figs. S3 and S4).

Post-hoc comparison of circulating biomarkers demonstrated that CK18 was 87% higher in the obese NAFLD-MetS group compared with the lean control group (166 ± 110 U/L vs. 88 ± 25 U/L, $p < 0.001$) and 46% higher compared with the obese control group (166 ± 110 U/L vs. 113 ± 41 U/L, $p = 0.019$; Fig. 4a). Furthermore, CK18 was 28% higher in the obese control group compared with the lean control group (113 ± 41 U/L vs. 88 ± 25 U/L, $p = 0.017$; Fig. 4a). On the other hand, no significant differences were observed between either group when assessing TIMP1 (Fig. 4b) or PIINP (Fig. 4c). The same patterns were observed for all three biomarkers when grouping according to the MASLD criteria (Fig. S5).

Finally, the post-hoc analysis investigating fibrosis algorithms showed that the FIB-4 index was 26% higher in the lean control group compared with the obese control group (1.0 ± 0.4 vs. 0.8 ± 0.2 , $p = 0.029$; Fig. 5a). Next,

Characteristic	Group			P value
	Lean control	Obese control	Obese NAFLD-MetS	
General				
Age	45.9 (8.1)	43.8 (7.0)	48.1 (7.1)	0.094
BMI (kg/m^2) ^a	22.8 (1.6)	35.2 (2.9)	36.0 (2.8)	<0.001
Platelets ($10^9/\text{l}$) ^a	221 (36.8)	268 (53.7)	253 (47.2)	0.002
Female/Male ^b	15 (55.6)/12 (44.4)	22 (78.6)/6 (21.4)	18 (54.5)/15 (45.5)	0.104
Liver enzymes				
ALT (U/L) ^a	23.0 (11.7)	22.4 (10.2)	33.8 (16.0)	0.003
AST (U/L) ^a	21.5 (5.0)	22.2 (6.1)	25.4 (7.3)	0.050
Lipids				
Triglycerides (mmol/L) ^a	0.9 (0.4)	1.1 (0.4)	1.6 (0.7)	<0.001
HDL (mmol/L) ^a	1.5 (0.4)	1.3 (0.3)	1.2 (0.2)	<0.001
LDL (mmol/L) ^a	2.8 (0.7)	2.8 (0.7)	3.0 (0.8)	0.426
Cholesterol (mmol/L) ^a	4.7 (0.9)	4.6 (0.8)	4.9 (0.9)	0.440
Metabolism				
Glucose (mmol/L) ^a	5.2 (0.3)	5.3 (0.4)	5.9 (0.5)	<0.001
Insulin (pmol/L) ^a	38.7 (17.5)	74.0 (22.4)	155.6 (72.6)	<0.001
GGT (U/L) ^a	17.6 (7.3)	25.1 (16.6)	38.9 (24.4)	<0.001
HOMA2-IR ^a	0.8 (0.4)	1.6 (0.5)	3.4 (1.5)	<0.001
HbA _{1C} (mmol/mol) ^a	32.4 (2.8)	33.5 (3.7)	35.4 (3.3)	0.002
Other				
Liver steatosis (%) ^a	2.1 (0.8)	3.4 (2.5)	12.9 (8.5)	<0.001
NAFLD ^b	0 (0)	3 (10.7)	33 (100)	<0.001
MetS components				
Blood pressure ^b	12 (44.4)	19 (67.9)	33 (100)	<0.001
Central obesity ^b	3 (11.1)	28 (100)	33 (100)	<0.001
Glucose ^b	2 (7.4)	7 (25.0)	26 (78.8)	<0.001
HDL ^b	2 (7.4)	10 (35.7)	21 (63.6)	<0.001
Triglycerides ^b	2 (7.4)	3 (10.7)	14 (42.4)	<0.001

Table 1. Clinical and metabolic features of study individuals according to study group. GGT gamma-glutamyltransferase, HbA1C glycated haemoglobin, HDL high-density lipoprotein, HOMA2-IR homeostasis model assessment 2 for insulin resistance, LDL low-density lipoprotein, NAFLD non-alcoholic fatty liver disease, MetS metabolic syndrome. ^aMean (SD). ^bn (%).

the Forns score was 15% higher in the obese NAFLD-MetS group compared with the obese control group (6.6 ± 0.8 vs. 5.8 ± 0.9 , $p=0.003$) and 9% higher in lean control group compared with the obese control group (6.3 ± 0.9 vs. 5.8 ± 0.9 , $p=0.042$; Fig. 5b). FNI was 256% higher in the obese NAFLD-MetS group compared with the lean control group ($15 \pm 12\%$ vs. $6 \pm 4\%$, $p<0.001$) and 75% higher compared with the obese control group ($15 \pm 12\%$ vs. $9 \pm 7\%$, $p=0.018$ Fig. 5c). Finally, we found that the MACK3 score was nearly 4 times higher in the obese NAFLD-MetS group compared with the obese control group (0.18 ± 0.15 vs. 0.05 ± 0.04 , $p<0.001$) and around 9 times higher compared with the lean control group (0.18 ± 0.15 vs. 0.02 ± 0.02 , $p<0.001$). Finally, the MACK3 score was 256% higher in the obese control group compared with the lean control group (0.05 ± 0.04 vs. 0.02 ± 0.02 , $p=0.002$; Fig. 5d). When grouping by the MASLD criteria, similar differences were seen for the FIB-4 index (Fig. S6a), the FNI algorithm (Fig. S6c), and the MACK3 score (Fig. S6d), while the Forns score did not differ significantly between the two control groups (Fig. S6b).

Associations between CK18, FNI, T1 relaxation times, and the MACK3 score

Investigating associations between CK18, FNI, and T1 relaxation times, we found that several markers correlated. CK18 correlated with both FNI ($r=0.69$, $p<0.001$; Fig. 6a), and T1 relaxation times ($r=0.41$, $p<0.001$; Fig. 6b). Furthermore, FNI correlated with T1 relaxation times ($r=0.33$, $p=0.005$; Fig. 6c). Finally, we found that the MACK3 score correlated with T1 relaxation times ($r=0.50$, $p<0.001$; Fig. 6d) and FNI ($r=0.80$, $p<0.001$; Fig. 6e). Similar findings were observed when grouping according to the MASLD criteria (Fig. S7).

Discussion

We investigated early indicators of the presence of developing liver fibrosis in obese individuals with NALFD and MetS using a combination of established and novel non-invasive MRI imaging, circulating biomarkers, and liver fibrosis algorithms. Our key findings were that CK18, T1 relaxation time, FNI, and MACK3 were increased in obese individuals with NAFLD and MetS without clinical signs of advanced liver fibrosis and/or

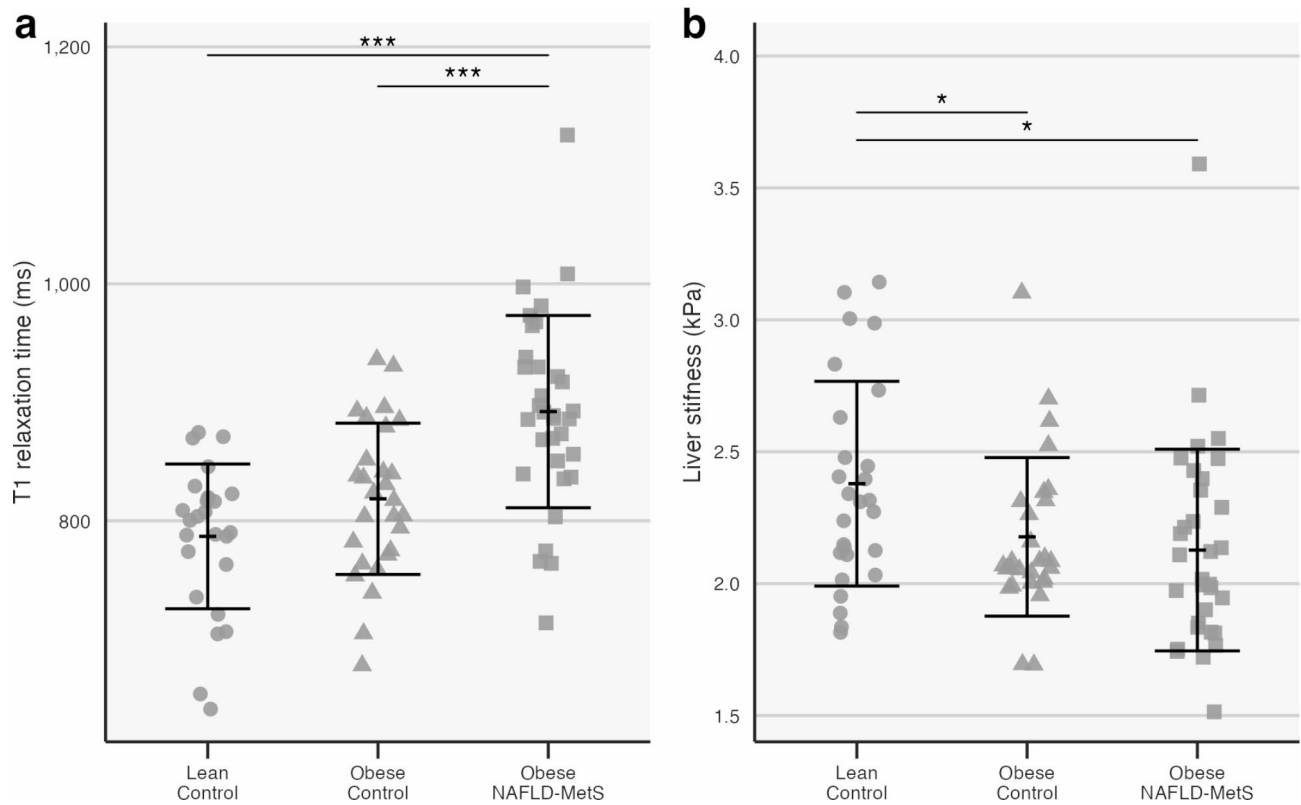


Fig. 2. Dot plots showing T1 relaxation times and liver stiffness (measured by MRE). **(a)** T1 relaxation times in Lean control group ($n=26$), Obese control group ($n=28$), and Obese NAFLD-MetS group ($n=33$). **(b)** Liver stiffness in Lean control group ($n=27$), Obese control group ($n=28$), and Obese NAFLD-MetS group ($n=32$). Error bars: Mean \pm SD. Significance levels: *(p value < 0.05), **(p value < 0.01), ***(p value < 0.001). MRE magnetic resonance elastography.

T2D. Additionally, we found correlation of these independent measures of liver fibrosis, which strongly suggest a beneficial use of these methods for non-invasive and early prediction of liver fibrosis risk in obese individuals.

Screening of large populations for liver fibrosis by biopsy is ineligible due to the multitude of risks and limitations¹¹. This leads to diagnosis of liver fibrosis focusing mainly on targeted populations, such as individuals with T2D or overt liver pathology^{35,36}. However, liver fibrosis can occur without apparent liver disease and in accordance with our findings, Wong et al. found that the general population of Hong Kong presented with advanced liver fibrosis (by transient elastography) in 3.7% of individuals with NAFLD and 1.5% of individuals with normal ALT, highlighting the occurrence of liver fibrosis without any overt signs. While Wong et al. only investigated severe fibrosis, it is likely that low grade fibrosis is even more prevalent³⁷. Moreover, studies that have investigated liver fibrosis in obese individuals without established liver pathology, have commonly utilized transient elastography, which is non-invasive but limited in its ability to detect low-grade fibrosis^{38–40}. Newer methods such as T1 mapping, MRE, TIMP1, CK18, FNI, and Forns scores offer higher sensitivity and have been suggested for identifying the early stages of fibrosis and fibroinflammation (MACK3)^{24,30,41,42}.

Qadri et al. did a comprehensive investigation of several fibrosis biomarkers in obesity and their dependence of BMI in relation to later stages of liver fibrosis, reporting advantages of combining markers to increase specificity³⁰. Our study is the first to provide a comprehensive characterization and comparison including eight different liver fibrosis markers, showing elevated T1 mapping, CK18, FNI, and MACK3 in obese individuals with NAFLD and MetS (or MASLD) compared with obese individuals with none or only one of these conditions. Combined, these results underline the need for further research on the prevalence and diagnosis of emerging liver fibrosis in non-targeted obese populations and the potential utility of non-invasive methods for the identification of individuals at risk (stratification according to a metabolic obesity phenotype).

MRI-based biomarkers, such as T1 mapping and MRE, have been shown to efficiently identify liver fibrosis and cirrhosis^{15,43,44}. In example, Hoffman et al. found that T1 mapping and MRE strongly correlated with liver fibrosis and could predict severe liver fibrosis in patients with known (by liver biopsy) or suspected liver disease (with an area under the receiver operator curve (AUROC) between 0.67 and 0.97, respectively)¹⁴. To this end, our findings showing higher T1 relaxation times in the obese NAFLD-MetS group indicate association with elevated liver fibrosis risk. However, our MRE data show lower liver stiffness in the obese NAFLD-MetS group and thus, a negative association between liver stiffness and liver steatosis. This contradicts previous studies suggesting that steatosis does not affect MRE^{45,46}. We speculate that since our study only includes participants

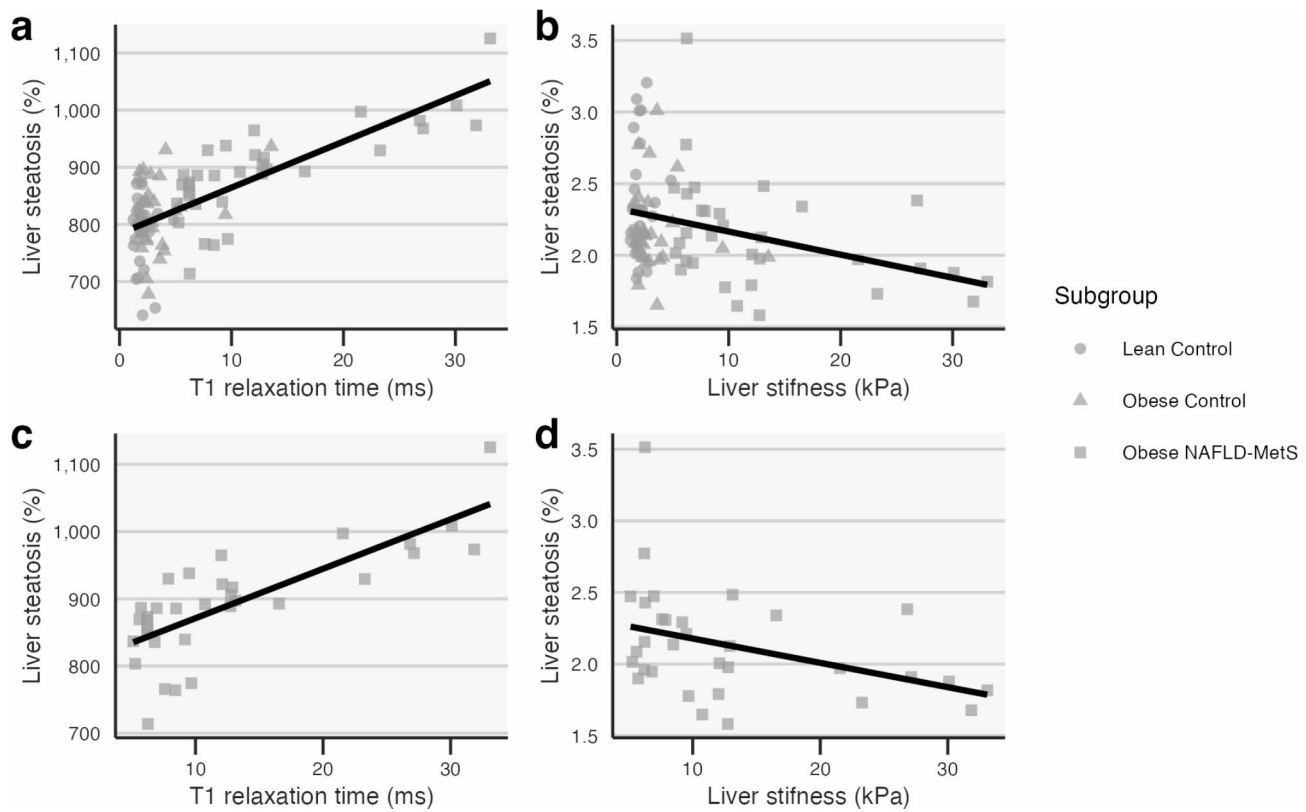


Fig. 3. Scatter plot showing associations of T1 relaxation times and liver stiffness with liver steatosis in the three study groups combined (**a,b**) and in the Obese NAFLD-MetS group (**c,d**). **(a)** Associations between T1 relaxation times ($n=87$) and liver steatosis ($n=88$), **(b)** associations between liver stiffness ($n=87$) and liver steatosis ($n=88$), **(c)** associations between T1 relaxation times ($n=33$) and liver steatosis ($n=33$), and **(d)** associations between liver stiffness ($n=32$) and liver steatosis ($n=33$). MRE magnetic resonance elastography.

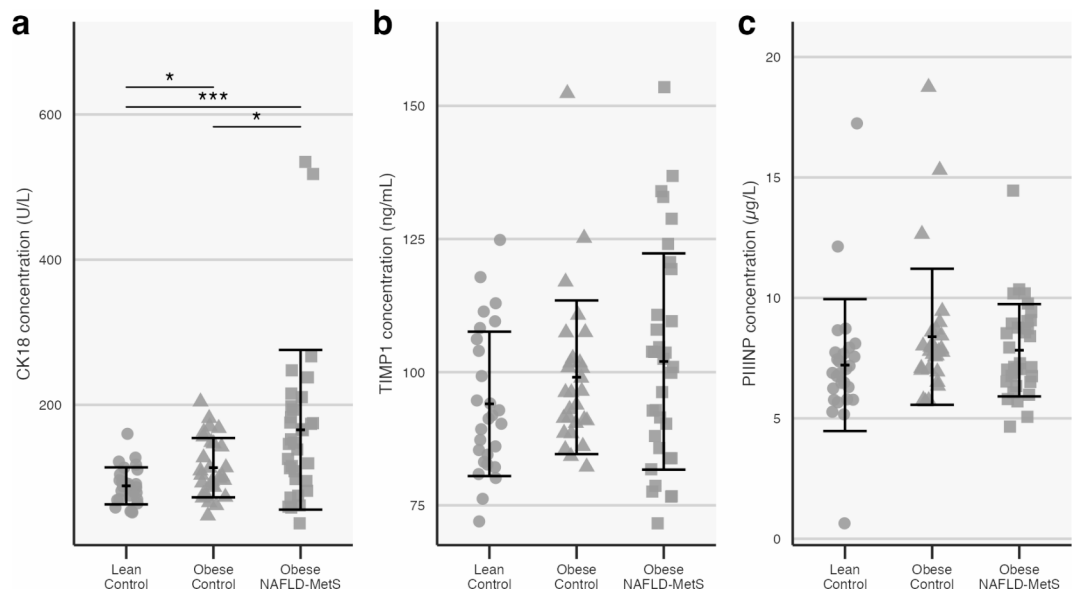


Fig. 4. Dot plots showing levels of the circulating biomarkers CK18, TIMP1, and PIIINP in Lean control group ($n=27$), Obese control group ($n=28$), and Obese NAFLD-MetS group ($n=33$). **(a)** CK18 levels in U/L. **(b)** TIMP1 levels in ng/mL, and **(c)** PIIINP levels in μ g/L. Error bars: Mean ± SD. Significance levels: *(p value < 0.05), **(p value < 0.01), ***(p value < 0.001). CK18 cytokeratin-18, PIIINP procollagen-III peptide, TIMP1 tissue inhibitor of metalloproteinases 1.

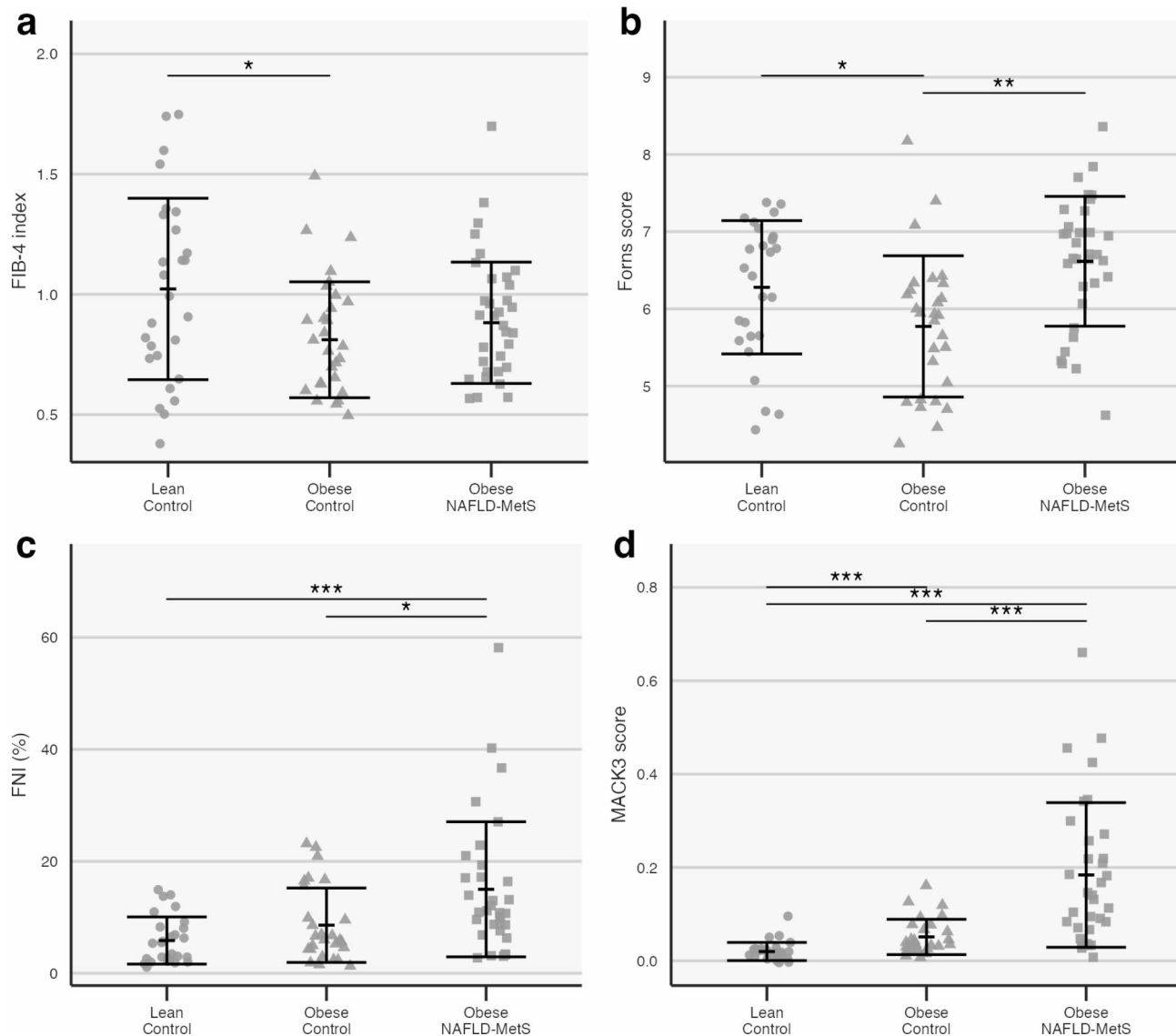


Fig. 5. Dot plots showing levels of the combination biomarkers FIB-4 index, Forns score, FNI, and MACK3 score in Lean control group ($n=27$), Obese control group ($n=28$), and Obese NAFLD-MetS group ($n=33$). **(a)** the FIB-4 index, **(b)** the Forns score, **(c)** FNI scores in %, and **(d)** MACK3 scores. Error bars: Mean \pm SD. Significance levels: *(p value < 0.05), **(p value < 0.01), ***(p value < 0.001). *FIB4-index* fibrosis-4 index, *FNI* fibrosis non-alcoholic steatohepatitis index.

without overt liver disease and expectedly no late-stage fibrosis, this apparent inverse relationship between liver steatosis and stiffness may reverse only in later stage fibrosis.

While MRI and MRE are non-invasive, their use for screening is often limited by high costs related to the need for specialized equipment and analysis. In contrast, circulating biomarkers, such as TIMP1, PIIINP, and CK18 are simple and inexpensive to measure, and thus excellent for screening larger populations^{17–19}. A hallmark of circulating biomarkers relates to their pronounced association with disease pathophysiology. For instance, TIMP1 is involved in degradation of the ECM, PIIINP is a pro-peptide that is detached from collagen, while CK18 is highly expressed in the liver (5% of total liver protein) and released from epithelial cells during injury and cell death^{18,47–49}. Our study identified no significant differences in TIMP1 and PIIINP levels, whereas CK18 was increased in the obese NAFLD-MetS group compared with the obese and lean control groups. Enhanced CK18 have been shown in NASH and likely increases the risk of liver fibrosis¹⁹. Hence, our findings could indicate that individuals with obesity, NAFLD, and MetS have increased inflammation and hepatocyte injury, which could be indicative of emerging liver fibrosis.

The progression of liver fibrosis from NAFLD involves lipotoxicity and damaged hepatocytes that drives oxidative stress and tissue inflammation. Subsequently, activation of hepatic stellate cells enhances inflammation and production of ECM⁵⁰. This complexity of liver fibrosis is likely not captured by assessing a single biomarker, why algorithms that combine several biological parameters increase the sensitivity for detection, especially in

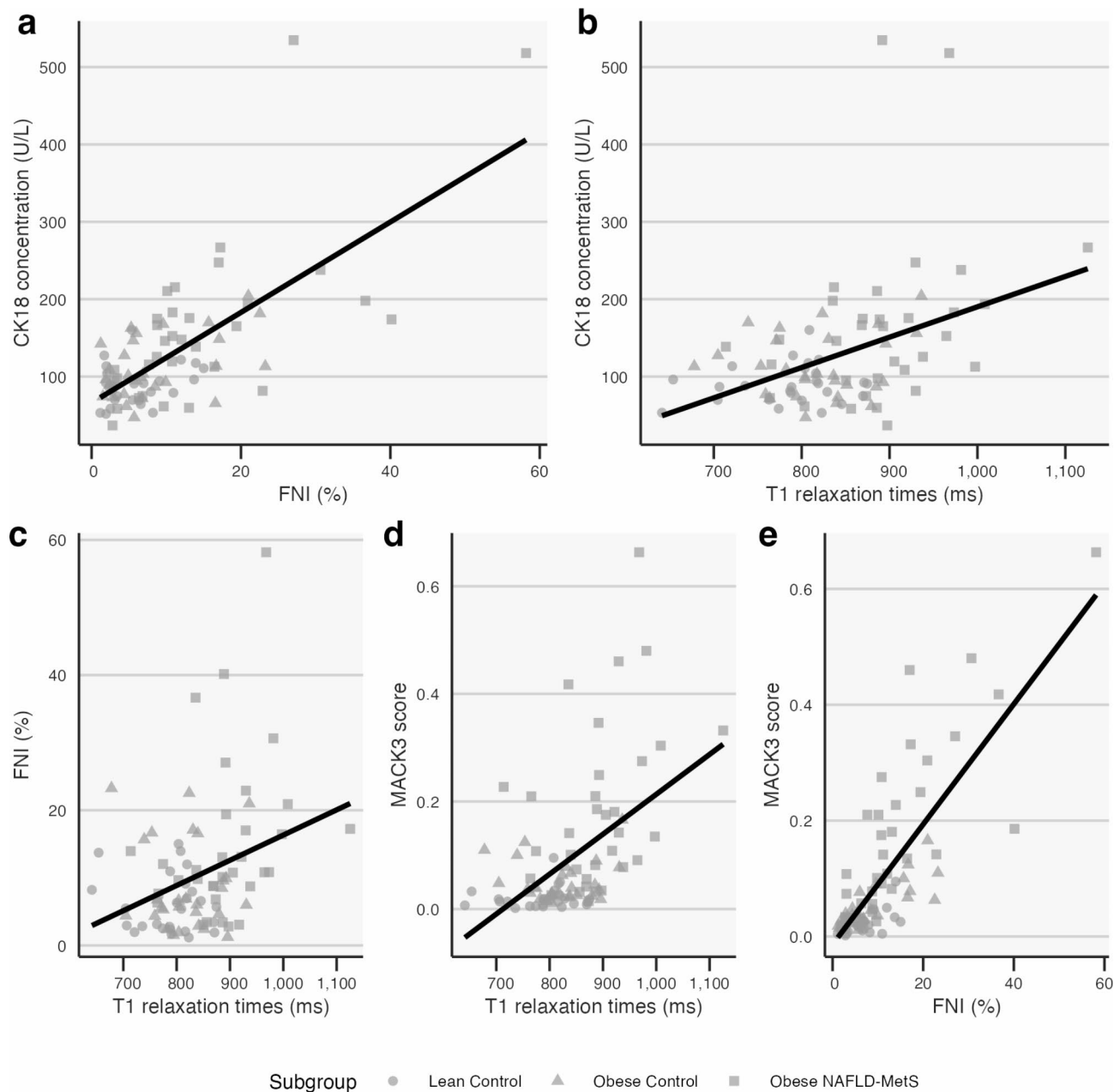


Fig. 6. Scatter plots showing associations between CK18, FNI, T1 relaxation times, and MACK3 score: (a) CK18 ($n=88$) and T1 relaxation times ($n=87$), (b) CK18 ($n=88$) and FNI ($n=88$), (c) FNI ($n=88$) and T1 relaxation times ($n=87$), (d) MACK3 score ($n=88$) and T1 relaxation times ($n=87$), and (e) MACK3 score ($n=88$) and FNI ($n=88$). CK18 cytokeratin-18, FNI fibrosis non-alcoholic steatohepatitis index.

targeted populations with increased risk⁵¹. In example, the FIB-4 index include age, platelet count, ALT, and AST and is routinely used to identify individuals at high risk of severe liver fibrosis¹². Whereas recent biomarker algorithms like the Forns score and FNI have shown improved sensitivity towards early stages of liver fibrosis compared with the FIB-4 index²¹. Thus, our finding that FNI is increased in the obese NALFD-MetS group could indicate early signs of liver fibrosis risk. Interestingly, the MACK3 score, which has validated cutoff values²⁴, are increased in 17 participants in the NAFLD-MetS group and one in the obese control group to a level (between 0.135 and 0.549) that places these individuals in “the grey zone”, suggesting the presence of active or fibrotic NASH.

Finally, studies have estimated that a Forns score above 6.9–7.1 predicts advanced liver fibrosis with 90% accuracy^{32,52}. Interestingly, we found that 23% of all participants had a Forns score above 7, suggesting a low specificity in our population. This, in conjunction with the Forns score being developed for identifying significant fibrosis in chronic hepatitis C patients, indicates that its use remains limited in obesity and NAFLD³².

Our study shows that obese individuals with NAFLD and MetS have higher levels of the various liver fibrosis biomarkers: T1 relaxation times, CK18 concentration, FNI, and MACK3 score. Importantly, the use of different and independent methods (except for CK18 and MACK3, since CK18 is part of the MACK3 algorithm), and their direct correlations strengthens our findings and suggestion that an evident liver fibrosis risk can be detected in obese individuals with NAFLD and MetS, prior to clinical signs of liver fibrosis. Moreover, the observed increase in T1 relaxation times and decrease in liver stiffness, may suggest earlier stages of liver fibrosis, such as fibroinflammation, which is further supported by our data showing FIB-4 index values below commonly used cut-off values for predicting advanced liver fibrosis. However, since we lack liver biopsy analysis, we cannot surely establish the potential presence or grade of liver fibrosis in our study participants, but merely estimate a latent risk. More studies are needed to further investigate and potentially establish the use of these biomarkers for early identification of liver fibrosis risk in obese individuals with NAFLD and MetS.

Obesity is a heterogeneous condition with varying degrees of metabolic complications^{31,53} why early risk stratification is essential. Few studies have investigated the association between obesity phenotype and liver fibrosis risk^{38,39,54}, although insight into early onset and thus assessment prior to clinical signs using non-invasive tools is sparse. We present data showing increased levels of liver fibrosis biomarkers when grouping obese individuals based on the presence of both NAFLD and MetS or according to the newly recommended MASLD criteria³⁴. Since our original study design, focusing on both NAFLD and MetS, is very close to the MASLD definition, we found only one difference between the two grouping strategies (the Forns score differed between the two control groups for MASLD grouping). Studies that directly compare NAFLD and MASLD would shed more light on the weight of the MetS parameters contained within MASLD and offer invaluable insight into obesity phenotyping based on metabolic risk and how this could enable improved obesity management if implemented in clinical settings.

By utilizing a variety of non-invasive liver fibrosis biomarkers, we provide a comparison of various methods that increase the validity of our findings that individuals with obesity, NAFLD, and MetS have increased markers of liver fibrosis. However, the lack of liver biopsies for confirmation and staging of fibrosis is a significant limitation, which limits the certainty of our findings. Furthermore, while several studies provide cut-off values for diagnosis of liver fibrosis, most were not eligible in our study as none of our participants (by study design) suffered from apparent liver fibrosis. To this end, our conclusion is based on established biomarkers related to overt and emerging liver fibrosis. In addition, the low sample size of the groups in our study is a limitation that may constrain its statistical power and generalizability and necessitates careful interpretation of our findings. However, the pronounced effect sizes observed in most of our presented findings suggest that the impact of sample size might be less critical in this context. Furthermore, we show every data point and share reproducible statistical code, allowing for independent evaluation of the findings. Finally, our study is limited by the lack of data on lifestyle would have shed an important light on our findings.

In conclusion, this study provides an extensive evaluation of a broad range of independent biomarkers of liver fibrosis in obesity and hereby add to the growing body of evidence on how to assess early liver fibrosis risk in a non-invasive manner. Our study hereby, provides novel insight into the expression levels of circulating levels of CK18, calculated MACK3 and FNI scores, and T1 relaxation times being elevated in obese individuals with NAFLD and MetS (or MASLD) compared with obese control individuals. In particular, CK18 and the MACK3 score has potential as accessible measures with the potential to change future assessment of liver fibrosis risk in obesity. Larger clinical studies that include information on liver fibrosis presence and stage via liver biopsies are needed to further elaborate on our findings and determine use and potential reference values for use in “early NAFLD”. Moreover, since lifestyle, such as diet and physical activity, are important factors in developing NAFLD and MASLD including such aspects in future studies would provide additional insights. As such, we provide knowledge that categorizing obesity based on the presence of NAFLD and MetS (or MASLD) could provide a framework for managing obesity that considers the risk of developing advanced liver disease.

Methods

Study population

This study utilizes baseline data from the MULTISITE study conducted at Aalborg University Hospital (AAUH), Denmark (Fig. S8 and Table S7). The study is registered on ClinicalTrials.gov (NCT05699863), conducted in accordance with the Helsinki Declaration, and approved by the Health Ethics Committee of North Jutland, Denmark (N-20200013).

We screened 62 non-diabetic individuals with obesity and 35 lean weight individuals of similar age- and sex. In short, participants between 30 and 60 years were recruited from October 2020 to July 2022 and provided informed consent according to the study protocol prior to enrolment. Inclusion criteria were self-reported body mass index (BMI): for the lean control group between 18.5 and 25.0 kg/m² and for individuals with obesity between 30.0 and 40.0 kg/m² as well as motivation to participate in the weight-loss program, and absence of diabetes. Exclusion was based on: previously diagnosed diabetes or glycated haemoglobin (HbA_{1c}) > 48 mmol/mol; endocrine or malignant disease; pregnancy; alcohol abuse; drug abuse; contraindications to MRI scanning; ongoing medical treatment with corticosteroids, antibiotics, chemotherapy, and antibiotic treatment within two months prior to inclusion. Furthermore, lean control individuals were excluded if they presented with NAFLD ($\geq 5\%$ liver steatosis) assessed by MRI. We compared levels of liver fibrosis markers by three different, independent types of methods (MRI, circulating markers, and algorithms) for all three groups. We included 88 participants, including 61 non-diabetic individuals with obesity and 27 lean weight individuals (Fig. 1).

Study design

The current study is a case-control study designed to identify and quantify various metabolic risk factors among obese individuals with NAFLD and MetS (obese NAFLD-MetS group), obese individuals without or with either

NAFLD or MetS, but not both (obese control group), and lean individuals (lean control group). All participants underwent a baseline visit at AAUH that included blood sample collection, MRI, and collection of clinical data (anthropometry and blood pressure). Participants were requested to fast overnight (> 8 h) and remained fasting for the duration of the study visit. All assessments were completed in a single day to minimize confounding factors related to sample collection times. After the baseline visit, obese participants were grouped into an obese NAFLD-MetS group (with both NAFLD ($\geq 5.0\%$ liver steatosis) and MetS (according to the IDF criteria⁵: Presence of three or more of the following criteria: elevated waist circumference (≥ 94 cm in men or ≥ 80 cm in women), elevated blood pressure (systolic blood pressure ≥ 130 mmHg or diastolic blood pressure ≥ 85 mmHg or antihypertensive drug), elevated fasting plasma glucose (≥ 5.6 mmol/l (100 mg/dL) or glucose-lowering drugs), elevated triglycerides (≥ 1.7 mmol/l (150 mg/dL) or lipid-lowering drug), low HDL cholesterol (< 1.03 mol/l (40 mg/dL) in men or < 1.29 mmol/l (50 mg/dL) in women or lipid-lowering drug) or an obese control group (without or with either NAFLD or MetS, but not both) (Fig. S8).

Clinical data

Clinical measurements included weight (participants wearing a hospital gown), height (using a stadiometer), waist and hip circumference (according to the guidelines of the world health organization (WHO))⁵⁵. Blood pressure was measured a minimum of three times after a 5–10 min period of seated rest and reported as the average of the last two measurements.

Circulating biomarkers

Venous blood was collected by a trained biomedical laboratory technician using antecubital venepuncture with a 21- or 24-gauge needle. The collected blood was analysed immediately or aliquoted and stored at -80°C . Routine blood analysis was performed immediately after sample collection at an accredited hospital laboratory (DS/EN ISO 16189). Briefly, plasma glucose, alanine transaminase (ALT), aspartate transaminase (AST), gamma glutamyl transferase (GGT), cholesterol, high-density lipoproteins (HDL), triglycerides (TG), and C-reactive protein (CRP) were measured on Cobas 6000c (Roche, Mannheim, Germany). Low-density lipoproteins (LDL) were calculated using the Friedewald equation⁵⁶. Serum insulin and C-peptide levels were measured on Cobas 601E (Roche, Mannheim, Germany). Platelet concentration was measured on Sysmex XN-9000 (Sysmex Co., Kobe, Japan). HbA_{1c} was measured on Sebia Capillarys 3 (Sebia, Lisses, France). Insulin resistance was estimated using the homeostasis model assessment for insulin resistance (HOMA2-IR), and was calculated from specific insulin and fasting plasma glucose levels using the iterative structural model using the HOMA2 calculator (RRID: SCR_023419)^{57,58}.

TIMP1 was measured using Quantikine ELISA kit (R&D Systems Inc., Minneapolis, MN, USA, Cat. #DTM100, Lot. #651-170619, RRID: AB_2813877) and CK18 was measured using the M30 Apoptosense CK18 ELISA Kit (VLVbio, Stockholm, Sweden, Cat. #P10011, Lot. #10011-014, RRID: AB_2935871) following manufacturer's instructions. Serum PIIINP was measured in an accredited routine hospital laboratory (DS/EN ISO 16189) by the Atellica IM analysis (Siemens Healthineers, Erlangen, Germany). The inter-assay CVs for all ELISA are presented as supplementary material.

Liver fibrosis algorithms

Liver fibrosis algorithms were calculated for the FIB-4 index, Forns score, and FNI. The FIB-4 index was calculated using Eq. (1)²²:

$$FIB - 4 = \frac{Age (years) * AST (U/L)}{Platelets (10^9/L) * \sqrt{ALT (U/L)}} \quad (1)$$

The Forns score was calculated using Eq. (2)²³:

$$\begin{aligned} Forns score = & 7.811 - 3.131 * \ln(Platelets (10^9/L)) + 0.781 * \ln(GGT (U/L)) \\ & + 3.467 * \ln(Age (years)) - 0.014 * Cholesterol (mg/dL) \end{aligned} \quad (2)$$

FNI was calculated using Eq. (3)²¹:

$$FNI = \frac{e^{-10.33+2.54*\ln(ALT(U/L))+3.86*\ln(HbA1c(%))-1.66*\ln(HDL(mg/dL))}}{1 - e^{-10.33+2.54*\ln(ALT(U/L))+3.86*\ln(HbA1c(%))-1.66*\ln(HDL(mg/dL))}} * 100 \quad (3)$$

MACK3 was calculated according to²⁴, using the online MACK3 calculator⁵⁹. Because the MACK3 calculator requires insulin reported in $\mu\text{IU}/\text{mL}$, we converted insulin from pmol/L (collected unit) to $\mu\text{IU}/\text{mL}$ using the unit conversion for human insulin of $1 \mu\text{IU}/\text{mL} = 6.00 \text{ pmol/L}$.

Imaging

Liver steatosis was determined by MRI using proton density fat fraction (PDFF) and liver fibrosis was evaluated by MRI using T1 mapping and MRE. Participants were scanned in a 3T MRI scanner (Signa Premier, General Electric, Milwaukee, WI, USA) using a flexible 30-channel coil (AIR) and a 60-channel in-bed coil in the supine position. PDFF maps were obtained using breath-hold multi-point Dixon (IDEAL IQ) sequences using fat- and water-only images to generate PDFF maps⁶⁰. For T1 mapping, a pulse-triggered modified Look-Locker inversion recovery (MOLLI) 2D imaging sequence was done as described⁶⁰. MRE was performed using mechanical waves

centred on the xiphisternum and generated using a rigid, round, active pneumatic driver fastened to the upper abdomen and vibrated at 40 Hz. Settings used for image capture is presented as supplementary material.

Image processing

Liver steatosis was calculated from PDFF map images using Vitrea Read (v.8.3.53-55, Canon Medical Informatics Inc., Minnetonka, Minnesota, USA, RRID: SCR_023418) as the mean of four circular regions of interest (ROIs); (mean size: 10 cm²). Liver fibrosis was estimated using T1 mapping (T1 relaxation time) and MRE (liver stiffness). Assessment of T1 relaxation time was performed on the T1 maps using GE Volume Viewer (v. 15.0 Ext. 6, General Electrics, Milwaukee, WI, USA, RRID: SCR_023417), and calculated as the mean of four circular ROIs (mean size: 7 cm²). MRE was determined from stiffness maps generated using a direct inversion algorithm on the MRI scanner. Measurements were performed using GE Volume Viewer (v. 3.0, Ext. 2.3, General Electrics, Milwaukee, WI, USA, RRID: SCR_023417), and calculated as the mean of four circular ROIs (mean size: 9 cm²). ROIs for all measurements were placed in the anterior, posterior, medial, and lateral segments of the liver to include as much liver parenchyma as possible within the segments, excluding large vessels, the liver border, and artifacts, as recommended^{61,62}. Images were processed by a single skilled operator.

Data analysis

Hypotheses were tested using univariate statistics. Specifically, differences between continuous and categorical variables were tested using two-sided ANOVA (group differences) with the Benjamini–Hochberg procedure to correct for multiple comparisons. Variables with significant differences between groups were compared by post-hoc testing (pairwise comparison) using two-sided independent samples t-tests with the Holm–Bonferroni procedure to adjust for family-wise error rate. The relationships between two categorical variables were tested using the Chi-squared test. The ANOVA, independent samples t-test, and chi-square tests were conducted using simulated based inference testing, with permuted null distributions based on 3000 resamples. Variables with an observed statistic outside the simulated null distribution were assigned a *p* value of 0.00099. Associations between two continuous variables were tested using the Pearson correlation coefficient. The effect sizes of the associations were interpreted using Cohen's conventions⁶³. Statistical significance was defined as *p*<0.05 for all statistical analyses. Data are presented as means (SD) unless otherwise specified. Furthermore, to give the possibility of comparing liver fibrosis in MASLD, additional comparisons were conducted using an alternative grouping of MASLD, presented in supplementary materials.

Data processing, plotting, and statistical analyses were conducted using R version 4.3.3 (RRID: SCR_001905)⁶⁴. Information on the data analysis workflow and reproducible code is openly available at <https://doi.org/10.5281/zendo.6337195>. Supporting statistical results (observed statistic, unadjusted *p* values, and adjusted *p* values) are presented in supplementary Tables S2–S6 and Figs. S9–S13.

Data availability

Restrictions apply to the availability of some, or all data generated or analysed during this study to preserve patient confidentiality. The corresponding author will on request detail the restrictions and any conditions under which access to some data may be provided.

Received: 6 November 2024; Accepted: 3 January 2025

Published online: 27 March 2025

References

- Le, M.H. et al. 2019 Global NAFLD Prevalence: A Systematic Review and Meta-analysis. *Clin Gastroenterol Hepatol* (2021).
- Chooi, Y. C., Ding, C. & Magkos, F. The epidemiology of obesity. *Metabolism* **92**, 6–10 (2019).
- Trends in adult body-mass index in 200 countries from 1975 to 2014: a pooled analysis of 1698 population-based measurement studies with 19.2 million participants. *Lancet* **387**, 1377–1396 (2016).
- Fabbrini, E., Sullivan, S. & Klein, S. Obesity and nonalcoholic fatty liver disease: biochemical, metabolic, and clinical implications. *Hepatology* **51**, 679–689 (2010).
- Alberti, K.G., Zimmet, P. & Shaw, J. Metabolic syndrome--a new world-wide definition. A Consensus Statement from the International Diabetes Federation. *Diabet Med* **23**, 469–480 (2006).
- Cohen, J.C., Horton, J.D. & Hobbs, H.H. Human fatty liver disease: old questions and new insights. *Science (New York, N.Y.)* **332**, 1519–1523 (2011).
- Lazarus, J. V. et al. Advancing the global public health agenda for NAFLD: a consensus statement. *Nat Rev Gastroenterol Hepatol* **19**, 60–78 (2022).
- Network, G.B.o.D.C. Global Burden of Disease Collaborative Network. Global Burden of Disease Study 2019 (GBD 2019) Reference Life Table. 2021 [cited]
- Bataller, R. & Brenner, D. A. Liver fibrosis. *J Clin Invest* **115**, 209–218 (2005).
- Ratziu, V. et al. Sampling variability of liver biopsy in nonalcoholic fatty liver disease. *Gastroenterology* **128**, 1898–1906 (2005).
- EASL-ALEH Clinical Practice Guidelines. Non-invasive tests for evaluation of liver disease severity and prognosis. *J Hepatol* **63**, 237–264 (2015).
- Vallet-Pichard, A. et al. FIB-4: an inexpensive and accurate marker of fibrosis in HCV infection. comparison with liver biopsy and fibrotest. *Hepatology* **46**, 32–36 (2007).
- Castera, L., Forns, X. & Alberti, A. Non-invasive evaluation of liver fibrosis using transient elastography. *J Hepatol* **48**, 835–847 (2008).
- Hoffman, D. H. et al. T1 mapping, T2 mapping and MR elastography of the liver for detection and staging of liver fibrosis. *Abdom Radiol (NY)* **45**, 692–700 (2020).
- Li, Z. et al. Assessment of liver fibrosis by variable flip angle T1 mapping at 3.0T. *J Magn Reson Imaging* **43**, 698–703 (2016).
- Venkatesh, S. K., Yin, M. & Ehman, R. L. Magnetic resonance elastography of liver: technique, analysis, and clinical applications. *J Magn Reson Imaging* **37**, 544–555 (2013).
- Nie, Q. H. et al. Correlation between TIMP-1 expression and liver fibrosis in two rat liver fibrosis models. *World J Gastroenterol* **12**, 3044–3049 (2006).

18. Collazos, J. & Díaz, F. Role of the measurement of serum procollagen type III N-terminal peptide in the evaluation of liver diseases. *Clin Chim Acta* **227**, 37–43 (1994).
19. Feldstein, A. E. et al. Cytokeratin-18 fragment levels as noninvasive biomarkers for nonalcoholic steatohepatitis: a multicenter validation study. *Hepatology* **50**, 1072–1078 (2009).
20. Hemmann, S., Graf, J., Roderfeld, M. & Roeb, E. Expression of MMPs and TIMPs in liver fibrosis - a systematic review with special emphasis on anti-fibrotic strategies. *J Hepatol* **46**, 955–975 (2007).
21. Tavaglione, F. et al. Development and Validation of a Score for Fibrotic Nonalcoholic Steatohepatitis. *Clin Gastroenterol Hepatol* **21**, 1523–1532.e1521 (2023).
22. Sterling, R. K. et al. Development of a simple noninvasive index to predict significant fibrosis in patients with HIV/HCV coinfection. *Hepatology* **43**, 1317–1325 (2006).
23. Forns, X. et al. Identification of chronic hepatitis C patients without hepatic fibrosis by a simple predictive model. *Hepatology* **36**, 986–992 (2002).
24. Boursier, J. et al. Screening for therapeutic trials and treatment indication in clinical practice: MACK-3, a new blood test for the diagnosis of fibrotic NASH. *Aliment Pharmacol Ther* **47**, 1387–1396 (2018).
25. Simo, K. A. et al. Does a calculated “NAFLD fibrosis score” reliably negate the need for liver biopsy in patients undergoing bariatric surgery? *Obes Surg* **24**, 15–21 (2014).
26. Pimentel, S. K. et al. Evaluation of the nonalcoholic fat liver disease fibrosis score for patients undergoing bariatric surgery. *Arq Gastroenterol* **47**, 170–173 (2010).
27. Qureshi, K., Clements, R. H. & Abrams, G. A. The utility of the “NAFLD fibrosis score” in morbidly obese subjects with NAFLD. *Obesity surgery* **18**, 264–270 (2008).
28. Alqahtani, S. A. et al. Performance of Noninvasive Liver Fibrosis Tests in Morbidly Obese Patients with Nonalcoholic Fatty Liver Disease. *Obes Surg* **31**, 2002–2010 (2021).
29. Nassif, A. T. et al. Performance of the Bard Scoring System in Bariatric Surgery Patients with Nonalcoholic Fatty Liver Disease. *Obes Surg* **27**, 394–398 (2017).
30. Qadri, S. et al. Obesity Modifies the Performance of Fibrosis Biomarkers in Nonalcoholic Fatty Liver Disease. *J Clin Endocrinol Metab* **107**, e2008–e2020 (2022).
31. Stefan, N., Häring, H. U., Hu, F. B. & Schulze, M. B. Metabolically healthy obesity: epidemiology, mechanisms, and clinical implications. *Lancet Diabetes Endocrinol* **1**, 152–162 (2013).
32. Blüher, M. Metabolically Healthy Obesity. *Endocr Rev* **41** (2020).
33. Marchesini, G. et al. Nonalcoholic fatty liver, steatohepatitis, and the metabolic syndrome. *Hepatology* **37**, 917–923 (2003).
34. Rinella, M. E. et al. A multisociety Delphi consensus statement on new fatty liver disease nomenclature. *Hepatology* **78**, 1966–1986 (2023).
35. Chiang, D. J., Pritchard, M. T. & Nagy, L. E. Obesity, diabetes mellitus, and liver fibrosis. *Am J Physiol Gastrointest Liver Physiol* **300**, G697–702 (2011).
36. Liu, B., Balkwill, A., Reeves, G. & Beral, V. Body mass index and risk of liver cirrhosis in middle aged UK women: prospective study. *Bmj* **340**, c912 (2010).
37. Wong, V. W. et al. Prevalence of non-alcoholic fatty liver disease and advanced fibrosis in Hong Kong Chinese: a population study using proton-magnetic resonance spectroscopy and transient elastography. *Gut* **61**, 409–415 (2012).
38. Tutunchi, H. et al. Metabolically healthy and unhealthy obesity and the progression of liver fibrosis: A cross-sectional study. *Clin Res Hepatol Gastroenterol* **45**, 101754 (2021).
39. Kim, Y. et al. Metabolically healthy versus unhealthy obesity and risk of fibrosis progression in non-alcoholic fatty liver disease. *Liver Int* **39**, 1884–1894 (2019).
40. Talwalkar, J. A., Kurtz, D. M., Schoenleber, S. J., West, C. P. & Montori, V. M. Ultrasound-based transient elastography for the detection of hepatic fibrosis: systematic review and meta-analysis. *Clin Gastroenterol Hepatol* **5**, 1214–1220 (2007).
41. Motola, D. L., Caravan, P., Chung, R. T. & Fuchs, B. C. Noninvasive Biomarkers of Liver Fibrosis: Clinical Applications and Future Directions. *Curr Pathobiol Rep* **2**, 245–256 (2014).
42. Canivet, C. M. et al. Validation of the Blood Test MACK-3 for the Noninvasive Diagnosis of Fibrotic Nonalcoholic Steatohepatitis: An International Study With 1924 Patients. *Clin Gastroenterol Hepatol* **21**, 3097–3106.e3010 (2023).
43. Erden, A. et al. MRI quantification techniques in fatty liver: the diagnostic performance of hepatic T1, T2, and stiffness measurements in relation to the proton density fat fraction. *Diagn Interv Radiol* **27**, 7–14 (2021).
44. Rustogi, R. et al. Accuracy of MR elastography and anatomic MR imaging features in the diagnosis of severe hepatic fibrosis and cirrhosis. *J Magn Reson Imaging* **35**, 1356–1364 (2012).
45. Chen, J. et al. Liver stiffness measurement by magnetic resonance elastography is not affected by hepatic steatosis. *Eur Radiol* **32**, 950–958 (2022).
46. Yin, M. et al. Assessment of hepatic fibrosis with magnetic resonance elastography. *Clin Gastroenterol Hepatol* **5**, 1207–1213.e1202 (2007).
47. Korver, S. et al. The application of cytokeratin-18 as a biomarker for drug-induced liver injury. *Arch Toxicol* **95**, 3435–3448 (2021).
48. Murawaki, Y., Ikuta, Y., Idobe, Y., Kitamura, Y. & Kawasaki, H. Tissue inhibitor of metalloproteinase-1 in the liver of patients with chronic liver disease. *J Hepatol* **26**, 1213–1219 (1997).
49. Schutte, B. et al. Keratin 8/18 breakdown and reorganization during apoptosis. *Exp Cell Res* **297**, 11–26 (2004).
50. Hernandez-Gea, V. & Friedman, S. L. Pathogenesis of liver fibrosis. *Annu Rev Pathol* **6**, 425–456 (2011).
51. Hagström, H., Talbäck, M., Andreasson, A., Walldius, G. & Hammar, N. Ability of Noninvasive Scoring Systems to Identify Individuals in the Population at Risk for Severe Liver Disease. *Gastroenterology* **158**, 200–214 (2020).
52. Bukhari, T. et al. Diagnostic Accuracy of the Forns Score for Liver Cirrhosis in Patients With Chronic Viral Hepatitis. *Cureus* **13**, e14477 (2021).
53. Karelis, A. D. et al. The metabolically healthy but obese individual presents a favorable inflammation profile. *J Clin Endocrinol Metab* **90**, 4145–4150 (2005).
54. Gutiérrez-Grobe, Y. et al. Less liver fibrosis in metabolically healthy compared with metabolically unhealthy obese patients with non-alcoholic fatty liver disease. *Diabetes Metab* **43**, 332–337 (2017).
55. World Health Organization. Waist circumference and waist-hip ratio: Report of a WHO expert consultation, Geneva, 8–11 December 2008. (2011) <https://apps.who.int/iris/handle/10665/44583> [Accessed May 30, 2022]
56. Friedewald, W. T., Levy, R. I. & Fredrickson, D. S. Estimation of the concentration of low-density lipoprotein cholesterol in plasma, without use of the preparative ultracentrifuge. *Clin Chem* **18**, 499–502 (1972).
57. Levy, J. C., Matthews, D. R. & Hermans, M. P. Correct homeostasis model assessment (HOMA) evaluation uses the computer program. *Diabetes Care* **21**, 2191–2192 (1998).
58. Hines, G., Kennedy, I., Holman R. HOMA2 Calculator. <https://www.dtu.ox.ac.uk/homacalculator/> [Accessed October 21, 2022]
59. Boursier, J. MACK3 Calculator. <http://forge.info.univ-angers.fr/~gh/wstat/mack3-calculator.php> [Accessed September 1, 2024]
60. Steinkohl, E., Olesen, S. S., Hansen, T. M., Dreves, A. M. & Frøkjær, J. B. T1 relaxation times and MR elastography-derived stiffness: new potential imaging biomarkers for the assessment of chronic pancreatitis. *Abdom Radiol (NY)* **46**, 5598–5608 (2021).
61. Campo, C. A. et al. Standardized Approach for ROI-Based Measurements of Proton Density Fat Fraction and R2* in the Liver. *AJR Am J Roentgenol* **209**, 592–603 (2017).

62. Hong, C. W. et al. Optimization of region-of-interest sampling strategies for hepatic MRI proton density fat fraction quantification. *J Magn Reson Imaging* **47**, 988–994 (2018).
63. J., C. *Statistical Power Analysis for the Behavioral Sciences*, 2nd ed. edn. New York: Routledge, 1988.
64. Team., R.C. R: A language and environment for statistical computing. [manual]. Vienna, Austria: R Foundation for Statistical Computing. (2022).

Acknowledgements

The authors would like to thank and acknowledge Anne-Mette Haubro Christensen, Birthe H. Thomsen, Rikke Bülow Eschen, and Zuzana Valnickova Hansen for collecting blood samples. Kenneth Krogh Jensen for assisting in planning and performing the MRI examinations. Merete Grothe Christensen, Mette Brodersen, Line Rosengreen Kaldahl, and Katrine Bruhn Vogensen for performing height and weight measurements, and Anne Lone Larsen for performing ELISA for TIMP1 and CK18.

Author contributions

Study conception and design: AH, AA, MM. Data collection: AA, AH, JBF, RWR, MG, MM. Analysis and interpretation of results: AA, AH, MM JBF, MG, KH. Draft manuscript preparation: AA, AH, MM. All authors reviewed the results and approved the final version of the manuscript.

Funding

This work was supported by a research grant from the Danish Diabetes Academy, which is funded by the Novo Nordisk Foundation, Grant No. NNF17SA0031406.

Declarations

Competing interests

The authors declare no competing interests.

Additional information

Supplementary Information The online version contains supplementary material available at <https://doi.org/10.1038/s41598-025-85508-y>.

Correspondence and requests for materials should be addressed to A.H.

Reprints and permissions information is available at www.nature.com/reprints.

Publisher's note Springer Nature remains neutral with regard to jurisdictional claims in published maps and institutional affiliations.

Open Access This article is licensed under a Creative Commons Attribution-NonCommercial-NoDerivatives 4.0 International License, which permits any non-commercial use, sharing, distribution and reproduction in any medium or format, as long as you give appropriate credit to the original author(s) and the source, provide a link to the Creative Commons licence, and indicate if you modified the licensed material. You do not have permission under this licence to share adapted material derived from this article or parts of it. The images or other third party material in this article are included in the article's Creative Commons licence, unless indicated otherwise in a credit line to the material. If material is not included in the article's Creative Commons licence and your intended use is not permitted by statutory regulation or exceeds the permitted use, you will need to obtain permission directly from the copyright holder. To view a copy of this licence, visit <http://creativecommons.org/licenses/by-nc-nd/4.0/>.

© The Author(s) 2025